Environmental Science and Ecotechnology 18 (2024) 100318

Contents lists available at ScienceDirect

Environmental Science and Ecotechnology

journal homepage: www.journals.elsevier.com/environmental-science-and-ecotechnology/

Original Research

Purple acid phosphatase promoted hydrolysis of organophosphate pesticides in microalgae

Xiang Wang [a, b], Guo-Hui He [a], Zhen-Yao Wang [c], Hui-Ying Xu [a], Jin-Hua Mou [b, d], Zi-Hao Qin [b, d], Carol Sze Ki Lin [b, *], Wei-Dong Yang [a], Yalei Zhang [e], Hong-Ye Li [a, **]

[a] Key Laboratory of Eutrophication and Red Tide Prevention of Guangdong Higher Education Institutes, College of Life Science and Technology, Jinan University, Guangzhou, 510632, China
[b] School of Energy and Environment, City University of Hong Kong, Tat Chee Avenue, Kowloon, Hong Kong
[c] Centre for Technology in Water and Wastewater, School of Civil and Environmental Engineering, University of Technology Sydney, Ultimo, NSW, 2007, Australia
[d] Southern Marine Science and Engineering Guangdong Laboratory (Guangzhou), Guangzhou, 510000, China
[e] State Key Laboratory of Pollution Control and Resources Reuse, College of Environmental Science and Engineering, Tongji University, Shanghai, 200092, China

ARTICLE INFO

Article history:
Received 26 January 2023
Received in revised form
24 August 2023
Accepted 13 September 2023

Keywords:
Biodegradation
Lipid accumulation
Organophosphate pesticide
Phaeodactylum tricornutum
Purple acid phosphatase

ABSTRACT

When organophosphate pesticides (OPs) are not used and handled in accordance with the current rules and standards, it results in serious threats to the aquatic environment and human health. *Phaeodactylum tricornutum* is a prospective microalgae-based system for pollutant removal and carbon sequestration. Genetically engineered *P. tricornutum*, designated as the OE line (endogenously expressing purple acid phosphatase 1 [PAP1]), can utilize organic phosphorus for cellular metabolism. However, the competencies and mechanisms of the microalgae-based system (namely the OE line of *P. tricornutum*) for metabolizing OPs remain to be addressed. In this study, the OE line exhibited the effective biodegradation competencies of 72.12% and 68.2% for 30 mg L^{-1} of dichlorvos and 50 mg L^{-1} of glyphosate, accompanied by synergistic accumulations of biomass (0.91 and 0.95 g L^{-1}) and lipids (32.71% and 32.08%), respectively. Furthermore, the biodiesel properties of the lipids from the OE line manifested a high potential as an alternative feedstock for microalgae-based biofuel production. A plausible mechanism of OPs biodegraded by overexpressed PAP1 is that sufficient inorganic P for adenosine triphosphate and concurrent carbon flux for the reduced form of nicotinamide adenine dinucleotide phosphate biosynthesis, which improved the OP tolerance and biodegradation competencies by regulating the antioxidant system, delaying programmed cell death and accumulating lipids via the upregulation of related genes. To sum up, this study demonstrates a potential strategy using a genetically engineered strain of *P. tricornutum* to remove high concentrations of OPs with the simultaneous production of biomass and biofuels, which might provide novel insights for microalgae-based pollutant biodegradation.

© 2023 The Authors. Published by Elsevier B.V. on behalf of Chinese Society for Environmental Sciences, Harbin Institute of Technology, Chinese Research Academy of Environmental Sciences. This is an open access article under the CC BY-NC-ND license (http://creativecommons.org/licenses/by-nc-nd/4.0/).

1. Introduction

Organophosphate pesticides (OPs) are commonly used as insecticides or herbicides in domestic and agricultural areas, and their daily use is expanding globally. China, being a major agricultural producer, has witnessed a surge in OP consumption and application [1]. Due to their cost-effectiveness and broad-spectrum effectiveness, OPs have gained a dominant market position, leading to extensive adoption by farmers. However, the World Health Organization has classified OPs as hazardous compounds due to their active groups of organophosphorus esters, necessitating strict control over their dosages. The improper management and overuse of OPs in response to insect and weed infestations in developing countries have been unsuccessful and possibly counterproductive [2]. Thousands of organophosphate poisoning cases

* Corresponding author.
** Corresponding author.
E-mail addresses: carollin@cityu.edu.hk (C.S.K. Lin), thyli@jnu.edu.cn (H.-Y. Li).

https://doi.org/10.1016/j.ese.2023.100318
2666-4984/© 2023 The Authors. Published by Elsevier B.V. on behalf of Chinese Society for Environmental Sciences, Harbin Institute of Technology, Chinese Research Academy of Environmental Sciences. This is an open access article under the CC BY-NC-ND license (http://creativecommons.org/licenses/by-nc-nd/4.0/).

were found in 2019 in Karachi, Pakistan, causing rapid clinical deterioration with minimal ingestion or exposure [3]. Moreover, unawareness and improper usage of OPs have led to their accumulation in agricultural and aquatic ecosystems, resulting in decreased water quality and global contamination of the oceanic environment [4,5]. With the increasing concentration of OPs from ng L^{-1} to μg L^{-1} levels in the marine environment, the exposure of marine organisms to OPs and the associated toxicological hazards have become virtually unavoidable [6–8]. Consequently, there is an urgent need for a systematic investigation of viable strategies to eliminate released OP pollutants from marine environments.

Numerous processes, such as oxidation, sedimentation, and absorption, have been investigated to remove OPs from aqueous environments. However, these strategies are time-consuming and labor-intensive, with toxic byproduct pollution and high energy consumption [9]. Moreover, these strategies do not align with the global sustainable development goals of a green, low-carbon economy. Microbial-based biodegradation of OPs has emerged as an attractive approach in recent years due to its advantages of low-cost and low-energy consumption, with high biodegradation efficiency [10–12]. Although several microorganisms possess biodegradation abilities, after treatment, microorganisms need to be processed into a harmless state using cumbersome procedures, potentially disrupting the environmental balance and even triggering secondary pollution [13,14]. Consequently, exploring a suitable organism for the efficient biodegradation of OPs in aqueous environments is urgent, especially in marine wastewater treatment containing OPs.

Microalgae, considered the most promising biological systems to achieve carbon peak and carbon neutrality, offer numerous advantages. They possess faster growth rates, simpler structures, and are abundant in biorefineries with high economic value, making them ideal for pollution treatment [15–18]. Among the various microalgal species, the diatom *Phaeodactylum tricornutum* is a viable alternative source for pollution treatment, with rapid growth and valuable product accumulation, thereby achieving the dual benefits of pollutant biodegradation and microalgal valorization [19,20]. The use of a low-carbon-emitting biological system like *P. tricornutum* for the biodegradation of organic pollutants is worth exploring. Studies have confirmed that *P. tricornutum* exhibits potential for the efficient removal of pollutants, such as triclosan and oxytetracycline, which are free of phosphorus (P) [21,22]; however, the removal efficiency of pollutants containing P by native *P. tricornutum* remains poor. Therefore, it is necessary to implement studies to improve the OP-biodegradation efficiency of *P. tricornutum*. Previous studies have reported that the continuing development and use of genome-editing tools for microalgae significantly broaden their abilities for the biodegradation and absorption of organic pollutants [23,24]. For instance, a *P. tricornutum* strain engineered with polyethylene terephthalate hydrolase (PETase) from *Ideonella sakaiensis* was generated successfully as an eco-friendly solution for biological PET degradation [25]. Moreover, the proof of principle that endogenous purple acid phosphatase 1 (PAP1) produced by an engineered *P. tricornutum* is functional for organophosphorus (i.e., adenosine triphosphate [ATP]) absorption and biodegradation under sole organic P conditions has been demonstrated [26]. However, the function of PAP1 in the biodegradation of environmentally hazardous organic P remains unknown. Therefore, it is crucial to investigate the effect of engineered *P. tricornutum* on OP removal, identify microalgal valorization by engineered *P. tricornutum*, and understand how this technique helps ameliorate the environmental impact of OPs. Moreover, the synergistic mechanism of PAP1 in OP biodegradation and valuable product accumulation remains to be explored.

To address these issues, two typical OP pollutants, dichlorvos, and glyphosate, were employed to investigate the potential for OP bioremediation by genetically engineered *P. tricornutum*, designated as the OE line in this study. We determined the tolerance and biodegradation competencies of high concentrations of OPs by the OE line of *P. tricornutum*. The effects of photosynthesis and recalibrated carbon flux were investigated to primarily explain the accumulations of biomass and lipids during the OP treatment. Thereafter, the biodiesel properties of biofuels extracted from the OE line were evaluated based on the proportions of fatty acids. Besides, the possible mechanism of improving OP tolerance and biodegradation competencies in the OE line was elucidated to understand how this technique can help ameliorate the environmental impact of OPs. Overall, these data uncovered a green and sustainable strategy for simultaneously biodegrading OPs and accumulating lipids in *P. tricornutum* by the endogenous overexpression of PAP1.

2. Materials and methods

2.1. Microalgal strain and maintenance

The wild-type strain (designated as the WT line) of *P. tricornutum* (Bacillariophyceae, SKU: CCMP2561) was purchased from the Provasoli-Guillard National Center for Marine Algae and Microbiota (East Boothbay, USA). The *P. tricornutum* strain overexpressing endogenous PAP1 (namely the OE line) was generated previously [26] and preserved at Jinan University (Guangzhou, China). The OE line was selected for OP treatment in this study due to its potential absorption and biodegradation capability of organic P.

All microalgae were maintained in 500 mL Erlenmeyer flasks with 400 mL of 0.22-μm-filtered natural seawater supplemented with f/2 medium. The WT and OE strains were cultured at 20 ± 1 °C in an artificial climate incubator with continuous cool white light at a light intensity of 200 μmol m^{-2} s^{-1} under a 12 h/12 h light/dark cycle with an initial inoculum of 1 × 10^6 cells mL^{-1}. All cultures were inoculated every seven days at a volume ratio 1:9 and harvested at specific time points for further analyses.

2.2. OP treatment of P. tricornutum

In the context of extensive global consumption, dichlorvos was widely used as an insecticide to control household pests, while glyphosate was a widely used herbicide to prevent overgrown weeds and grasses. Due to their widespread application, these two representative OPs were commonly detected in various environmental settings. To simulate real-world scenarios, we procured these commercially available OPs (purity ≥98%, PESTANAL grade) from Sigma-Aldrich (St. Louis, USA) for OP treatment of *P. tricornutum*. Briefly, two OPs were separately supplemented as the sole P source to replace the inorganic P ($NaH_2PO_4 \cdot H_2O$) in the original culture medium at final concentrations of 0, 10, 20, 30, 50, and 100 mg L^{-1} with seven-day treatment to evaluate the maximum biodegradation capabilities of PAP1-mediated *P. tricornutum*. All treatments were performed at least in triplicate, and the results were used to select the most suitable OP concentration for further experiments. The appropriate concentration of OPs (i.e., 30 mg L^{-1} of dichlorvos and 50 mg L^{-1} of glyphosate, respectively) was subsequently prepared for analytical experiments, as per the described sampling schedules, by centrifugation at 4400 rpm for 10 min. The schematic process of the methods used for this study is shown in Fig. 1a.

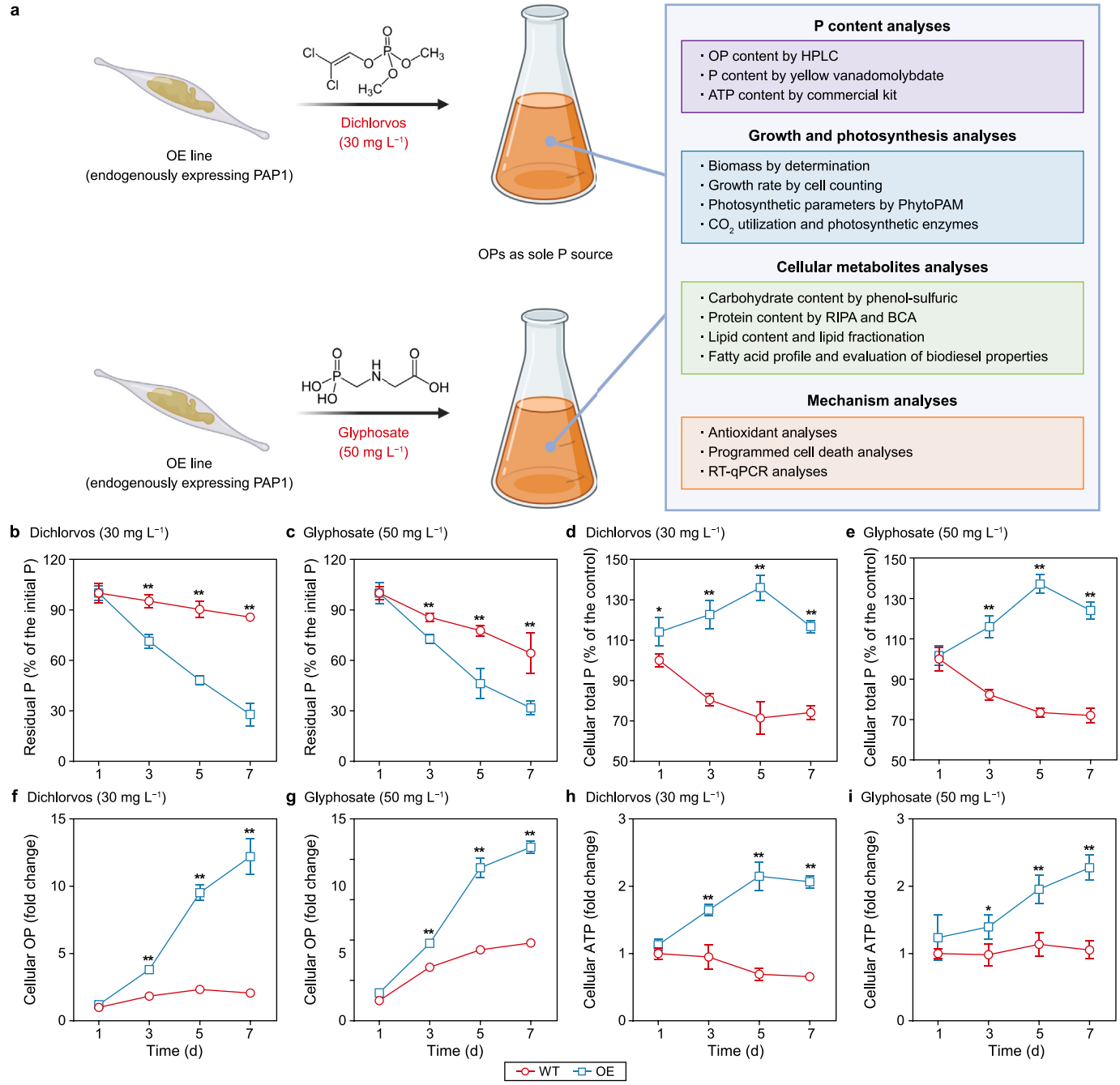

Fig. 1. **a**, Schematic progress of the methods used in this study. **b**–**c**, Analyses of the removal of OPs by the WT and OE lines of *P. tricornutum* cultures throughout the cultivation period. Residual P content of culture medium treated with 30 mg L^{-1} dichlorvos (**b**) or 50 mg L^{-1} glyphosate (**c**). **d**–**e**, Total P content of *P. tricornutum* cultures treated with 30 mg L^{-1} dichlorvos (**d**) or 50 mg L^{-1} glyphosate (**e**). **f**–**g**, OP content of *P. tricornutum* cultures treated with 30 mg L^{-1} dichlorvos (**f**) or 50 mg L^{-1} glyphosate (**g**). **h**–**i**, Intracellular ATP content of *P. tricornutum* cultures treated with 30 mg L^{-1} dichlorvos (**h**) or 50 mg L^{-1} glyphosate (**i**). Each error bar represents the standard deviation of three samples. A significant difference (*$p < 0.05$ and **$p < 0.01$) represents comparisons between the values of the WT and OE lines of *P. tricornutum* cultures.

2.3. P content analyses in P. tricornutum and culture medium treated with OPs

The concentrations of dichlorvos and glyphosate in both the microalgae and the culture medium were ascertained using a high-performance liquid chromatography system (HPLC, Agilent, USA) equipped with a reversed-phase C18 column and an ultraviolet–visible (UV–Vis) detector (Agilent, USA). For dichlorvos, the column was eluted at a flow rate of 0.8 mL min^{-1} using a mobile phase of acetonitrile and deionized water at a volume ratio of 60:40 for detection at the wavelength of 210 nm. For glyphosate, the column was eluted at a flow rate of 1.0 mL min^{-1} using a mobile phase prepared by mixing acetic acid (1%) with methanol at a volume ratio of 60:40 for detection at the wavelength of 254 nm. Analytic standards of dichlorvos and glyphosate (Sigma-Aldrich, USA) were used as references for quantification based on the normalization of the peak area. To determine the cellular OP content, 200 mL of WT and OE *P. tricornutum* cultures were collected and washed thrice with deionized water. Subsequently, microalgal pellets were ground in

liquid nitrogen for OP extraction with deionized water for subsequent HPLC analysis.

To determine the residual P content of the culture medium and the total cellular P content, the culture medium and microalgal pellets were transferred into clean ceramic crucibles for 5 h of combustion at 550 °C in a muffle furnace. After cooling, 2 mL of hydrochloric acid solution (2 N) was added to the ceramic crucibles for P extraction at room temperature for 30 min. The supernatant was then isolated by centrifugation at 15,000 rpm for 10 min for further P content determination following the standard protocols of the yellow vanadomolybdate method.

The cellular ATP content of WT and OE *P. tricornutum* cultures was determined using a commercial Plant ATP ELISA kit (Bangyi Biotech, China) following the manufacturer's instructions.

2.4. Biochemical and molecular analyses of P. tricornutum treated with OPs

2.4.1. Biomass determination

Approximately 100 mL of culture broth was collected and centrifuged at 4400 rpm for 10 min to obtain the microalgal pellets. Afterward, pellets were washed thrice with demineralized water and dried at 65 °C in an oven overnight to obtain the biomass by gravimetrical determination.

2.4.2. Growth and photosynthesis analyses

The cell density of the WT and OE lines during the OPs treatment period was directly counted with a Neubauer haemocytometer by using the Eclipse E200 optical microscope (Nikon, Japan). The specific growth rate (μ, d^{-1}) of *P. tricornutum* was calculated according to equation (1) as follows:

$$\mu\left(d^{-1}\right)=\frac{\ln N-\ln N_0}{t-t_0} \tag{1}$$

where N and N_0 represent the cell density of *P. tricornutum* cultures at the specific time points t and t_0, respectively.

Photosynthetic parameters, namely the maximum photochemical efficiency of photosystem II (Fv/Fm), the photosystem II-based electron transport rate (ETR), and non-photochemical quenching (NPQ) from WT and OE lines during the OP treatment period, were measured using a PhytoPAM II Phytoplankton & Photosynthesis Analyzer (Walz, Germany) as per the manufacturer's manuals.

The CO_2 utilization efficiency of *P. tricornutum* cultures was assessed using 500 mL Duran laboratory bottles with stainless steel two-port connector gaps and calculated based on the input and output quantities of CO_2 using gas chromatography (Shimadzu, Japan). Furthermore, for enzyme extraction, the centrifuged *P. tricornutum* pellets were ground in liquid nitrogen with the premixed solutions and the activities of two representative enzymes involved in photosynthesis, namely ribulose-1,5-bisphosphate carboxylase-oxygenase (RuBisCO) and carbonic anhydrase, were measured following previously reported protocols [27].

2.4.3. Primary metabolites analyses

Cellular carbohydrates were extracted from WT and OE *P. tricornutum* cultures following the standard protocols of the classic phenol-sulfuric method and were detected at the wavelength of 483 nm by UV–Vis spectrophotometry (Shimadzu, Japan). Cellular carbohydrate content was calculated based on the absorbance values normalized to a glucose standard curve. Cellular protein was isolated from WT, and OE *P. tricornutum* cultures using pre-cooled RIPA lysis buffer with protease inhibitor for 30 min and quantified at the wavelength of 562 nm by UV–Vis spectrophotometry (Shimadzu, Japan) using the Bicinchoninic Acid Kit for Protein Determination (Beyotime, China). Cellular protein content was calculated by referencing the absorbance value with the plotted bovine serum albumin standard curve.

Cellular lipids were isolated from WT and OE *P. tricornutum* cultures using an organic solvent extraction method with methanol, chloroform, and water. The isolated lipids were transferred to a pre-weighed 1.5 mL Eppendorf tube for drying under a nitrogen stream, and the content was further determined gravimetrically. Cellular triacylglycerol (TAG) was separated from the total lipids of *P. tricornutum* using thin-layer chromatography on a silica plate (Merck, Germany). Briefly, 20 μL of concentrated total lipids was spotted on a silica plate using capillary tubes. Furthermore, a developing solvent containing a mixture of hexane, diethyl ether, and acetic acid at a volume ratio of 85:15:1 was used to isolate TAG for 20–30 min at room temperature. Isolated TAG was visualized by iodine vapor in a sealed container and then scraped off into a new 1.5 mL Eppendorf tube containing chloroform. The solution was then vortexed for 5 min and centrifuged at 15,000 rpm for 10 min to separate the isolated TAG for further gravimetrical determination after drying under a nitrogen stream. The lipid profiles, including neutral lipid (NL), glycolipid (GL), and phospholipid (PL), were fractionated from total lipids using a solid–phase extraction column with pre-packed silica cartridges (Waters, USA) and further determined gravimetrically according to a previously published method [28].

2.4.4. Fatty acid profile analysis

WT and OE *P. tricornutum* lines were centrifuged at 4400 rpm for 10 min and transferred into a Teflon-lined screw-cap tube containing 500 μL of toluene. Afterward, 1 mL of fresh NaOH/Methanol (0.5 N) was added for mild vortex and subsequently incubated at 80 °C for 20 min. After cooling, 1 mL of the fresh premixed solvent containing acetyl chloride and methanol at a volume ratio 1:10 was slowly added along the tube wall and then incubated at 80 °C for 20 min. Furthermore, 1 mL of potassium carbonate solution (6%), 500 μL of hexane, and 10 μL of methyl nonadecylate (C19:0, internal standard) were added and mixed by mild vortex. The upper phase containing transesterified fatty acids (fatty acid methyl esters) was collected for further gas chromatography-mass spectrometry analysis after centrifugation at 2000 rpm for 10 min following previously published protocols [29].

2.4.5. Evaluation of biodiesel properties

To determine the quality of microalgae-based biofuels obtained from *P. tricornutum* treated with OPs, representative parameters, such as iodine value (IV), saponification value (SV), cetane number (CN), degree of unsaturation (DU), long-chain saturation factor (LCSF), high heating value (HHV), cold-flow plugging point (CFPP), kinematic viscosity (kV), and oxidative stability (OS), were evaluated based on the data of fatty acid profile using equations (2)–(10) as follows:

$$IV=\sum 254\times DB\times\frac{\%FC}{M} \tag{2}$$

$$SV=\sum 560\times\frac{\%FC}{M} \tag{3}$$

$$CN=46.3+\frac{5458}{SV}-(0.255\times IV) \tag{4}$$

$$DU\ (\%)=MUFA+(2\times PUFA) \tag{5}$$

$$LCSF = (0.1 \times C16) + (0.5 \times C18) \quad (6)$$

$$HHV = 49.43 - 0.041 \times SV - 0.015 \times IV \quad (7)$$

$$CFPP = (3.417 \times LCSF) - 16.477 \quad (8)$$

$$\ln(kV) = -12.503 + 2.496 \times \ln\left(\sum M\right) - 0.178 \times \sum DB \quad (9)$$

$$OS = \frac{117.9295}{(\%C18{:}2 + \%C18{:}3)} + 2.5905 \quad (10)$$

where *DB* represents the number of double bonds in each fatty acid profile; *M* represents the molecular weight of each fatty acid profile; *%FC* represents the percentage of each fatty acid profile in the total fatty acid content; *MUFA* and *PUFA* represent the molecular weight of monounsaturated fatty acid and polyunsaturated fatty acid, and *%C*18:2 and *%C*18:3 represent the molecular weight of C18:2 and C18:3, respectively.

2.4.6. Antioxidant analyses

Reactive oxygen species (ROS) were quantified based on the relative fluorescence intensity of *P. tricornutum* after staining with the cell-permeable probe 2′,7′-dichlorodihydrofluorescein diacetate (Beyotime, China), followed by fluorometric detection using a microplate reader (Bio-Tek, USA) at a 488 nm of excitation wavelength and a 500−600 nm range of emission wavelength. The reduced glutathione/oxidized glutathione (GSH/GSSG) ratio was monitored using the GSH/GSSG Ratio Detection Assay Kit II (Abcam, UK), with fluorometric detection using a microplate reader (Bio-Tek, USA) at an excitation wavelength of 490 nm and an emission wavelength of 520 nm. The activities of three representative antioxidant enzymes, namely glutathione peroxidase (GPx), superoxide dismutase (SOD), and catalase (CAT), were determined using the Cellular Glutathione Peroxidase Assay Kit with the reduced form of nicotinamide adenine dinucleotide phosphate (NADPH) (Beyotime, China), the Total Superoxide Dismutase Assay Kit with WST-8 (Beyotime, China), and the Catalase Assay Kit (Beyotime, China), respectively, following the manufacturer's standard protocols. The content of NADPH was determined using the NADPH Assay Kit (Abcam, UK), followed by colorimetric detection using a microplate reader (Bio-Tek, USA) at an absorption wavelength of 460 nm.

2.4.7. Programmed cell death analyses

Programmed cell death of *P. tricornutum* treated with OPs was assessed based on the externalization of phosphatidylserine (PS) residues, the activity of the caspase-3 protein, membrane permeability, and mitochondrial membrane potential. PS externalization examination in *P. tricornutum* cultures was performed using an eBioscience Annexin V-FITC Apoptosis Detection Kit (Invitrogen, USA) following the manufacturer's instructions, followed by the detection of positively stained cells using a flow cytometer (BD Biosciences, USA) at a 488 nm of excitation wavelength and a 520 nm of emission wavelength. According to the manufacturer's instructions, the caspase-3 protein activity of *P. tricornutum* cultures was determined using an EnzChek™ Caspase-3 Activity Assay Kit (Invitrogen, USA). The cellular membrane permeability of *P. tricornutum* cultures was analyzed based on staining with a propidium iodide solution (Sigma-Aldrich, USA), followed by fluorometric detection using a microplate reader (Bio-Tek, USA) at an excitation wavelength of 535 nm and an emission wavelength of 617 nm. Mitochondrial membrane potential was evaluated using a cationic carbocyanine dye (i.e., JC-1 dye solution, Abcam, UK) and then detected using a microplate reader (Bio-Tek, USA) at an excitation wavelength of 475 nm and an emission wavelength of 590 nm.

2.4.8. RT-qPCR analyses

The transcript abundance of eight genes, namely *PAP1*, four key death-related genes (heat shock protein 90, *HSP90*; death-specific protein, *DSP*; metacaspase, *MC*; programmed cell death, *PDCD*), and three critical lipid-related genes (glycerol-3-phosphate acyltransferase, *GPAT*; 1-acylglycerol-3-phosphate acyltransferase, *LPAT*; acyl-CoA:diacylglycerol acyltransferase, *DGAT*), was determined by reverse transcription-quantitative polymerase chain reaction (RT-qPCR) analysis. Briefly, total RNA was isolated from *P. tricornutum* using a Plant Total RNA Isolation Kit (Sangon, China) following the standard protocols. Subsequently, total RNA was transcribed into cDNA using HiScript II Q RT SuperMix for qPCR (Vazyme, China) following the manufacturer's instructions. RT-qPCR analyses were performed on a CFX96 Real-Time PCR Detection System (Bio-Rad, USA) using AceQ qPCR SYBR® Green Master Mix (Vazyme, China) in a final volume of 20 μL in eight-strip qPCR tubes. The data of RT-qPCR were normalized to the ribosomal protein small subunit 30S (*RPS*, reference gene) using the $2^{-\Delta\Delta Ct}$ method. All primers used in this study are listed in Table S1.

2.5. Statistical analysis

All experiments in this study were repeated at least three times, and the obtained results are expressed as means ± standard deviation. The data were plotted using GraphPad Prism 8 (GraphPad, USA). Differences between groups were investigated using a Kruskal−Wallis one-way analysis of variance, followed by Duncan's multiple range test. p values of <0.05 were considered statistical significance with different lowercase letters on the bars of columns. Differences between the WT and OE groups were determined using an unpaired Welch's t-test at a statistical significance of p values of <0.05 (*) or <0.01 (**).

3. Results and discussion

3.1. The OE line of P. tricornutum exhibited effective tolerance and biodegradation competencies for OP treatment

In *P. tricornutum*, the study revealed that PAP1 has multiple roles during the growth period. It promotes growth and photosynthesis through enhanced phosphate assimilation and increases lipid content during the late growth phase [26]. Besides, PAP1 plays a crucial role in potentiating reducing equivalents and Pi translocation through orchestrating the expression of Pi transporters [26]. However, the competencies of PAP1 for remediating environmentally hazardous organophosphorus pollutants (i.e., OPs) remained unknown. Therefore, the feasibility of using the PAP1-overexpression strain (namely the OE line) of *P. tricornutum* for efficient OP treatment should be determined. The OE line was retrieved from our previous report [26] and preserved at Jinan University (Guangzhou, China). As dichlorvos and glyphosate are representative OPs used to exterminate insects and weeds globally, we cultured *P. tricornutum* in the presence of a range of OP concentrations (0, 10, 20, 30, 50, and 100 mg L^{-1}) for seven days and evaluated the performance of *P. tricornutum* for OP treatment. It was found that the exposure to OPs over 20 mg L^{-1} exhibited growth inhibition to WT of *P. tricornutum* (Figs. S1a and b), revealing the toxicity of OPs to the native strain. However, the OE line of *P. tricornutum* exhibited tolerance when exposed to high concentrations of dichlorvos or glyphosate, with a higher growth rate than the WT line. In particular, the OE line treated with

30 mg L^{-1} dichlorvos or 50 mg L^{-1} glyphosate manifested the highest growth rate value at 0.26 or 0.29, respectively. These data demonstrate that the OE line of *P. tricornutum* tolerates a high concentration of OPs due to the overexpression of PAP1. It has been reported that an acid phosphatase from the aquatic plant, *Spirodela oligorrhiza*, is responsible for the nonspecific hydrolysis of several different OPs [30]. Similarly, purple acid phosphatase has been found to have a significant role in the bioremedial hydrolysis of OPs [31,32]. Accordingly, in the present study, the P content of the culture medium was measured to determine the OP-biodegradation potential of the OE line of *P. tricornutum*. As expected, the OP residue of the culture medium was found to be markedly lower in the OE line of *P. tricornutum* than in the WT line exposed to similar conditions, implying that the overexpression of PAP1 enhanced the OP-biodegradation ability of *P. tricornutum* (Figs. S1c and d). As shown in Fig. S2, the transcript level of PAP1 was significantly increased in the OE line when exposed to OPs. Likewise, it was reported that overexpression of endogenous PAP1 in *P. tricornutum* could contribute to the increase of PAP1 transcript level [26]. Similar reports have shown a strong positive correlation between phosphatase activity and OPs degradation in both prokaryotes and eukaryotes [33–35], which is in accordance with our findings of *PAP1* transcript abundance of *P. tricornutum* cultures (Fig. S2). In addition, significantly greater P absorption occurred in the OE line of *P. tricornutum* compared with the WT line when exposed to OPs (Figs. S1e and f). Therefore, as the OP exposure time increased, the OE line of *P. tricornutum* was stable to utilize OPs as the P source by hydrolyzing them into inorganic P under the pressure of inorganic P deficiency. These data demonstrate that the OE line of *P. tricornutum* retained the abilities of tolerance and biodegradation of OP pollutants. However, the OPs biodegradation and metabolic mechanism in the OE line of *P. tricornutum* required further analysis.

OPs biodegradation occurs via a first-order reaction, and the most effective enzyme for OP cleavage is phosphatase [36,37]. To investigate the details of OP metabolism, *P. tricornutum* cultures were treated with 30 mg L^{-1} dichlorvos or 50 mg L^{-1} glyphosate throughout the cultivation period to provide a comprehensive overview of the tolerance and biodegradation of OPs. Compared with the WT line, the OE line of *P. tricornutum* showed a stable and significant decrease in P concentration (up to 72.12% in the dichlorvos-treatment group and 68.2% in the glyphosate-treatment group) in the culture medium (Fig. 1b and c), suggesting that the successive removal of OPs and subsequent absorption of extracellular P occurred due to the overexpression of PAP1. This is consistent with the fact that the phosphatase enzyme caused the hydrolysis of organophosphate, leading to the release and absorption of organophosphate metabolites [36]. Moreover, PAP1 overexpression in the OE line caused a notable increase in cellular total P and OP content compared with their content in the WT line (Fig. 1d–g), which showed that the overexpression of acid phosphatase promoted the absorption of organic and inorganic P from the extracellular environment to the intracellular environment. Similarly, the cellular ATP concentration of *P. tricornutum* cultures was significantly elevated after PAP1 overexpression (Fig. 1h and i). These results agree with our previous study, which demonstrated that PAP1 overexpression enhanced cellular simple organic P uptake and degradation in *P. tricornutum*, thereby increasing the ATP concentration for microalgal metabolism [26]. Thus, these results suggest that PAP1 overexpression may be considered the main contributor to the improved ability of the OE line of *P. tricornutum* to hydrolyze and absorb high concentrations of complex OPs.

3.2. Enhanced photosynthesis in the OE line of P. tricornutum simultaneously contributed to the removal of OPs and the accumulation of biomass

Cultivation of the OE line of *P. tricornutum* in the presence of high concentrations of OPs resulted in a significant accumulation of biomass at 0.91 and 0.95 g L^{-1}, respectively (Fig. S3). This shows that PAP1 overexpression in *P. tricornutum* cultures is important in regulating biomass accumulation through intracellular P metabolism. The amount of microalgal photosynthesis has been found to positively correlate with the amelioration of pollutant removal and biomass accumulation [29]. Likewise, relevant studies have demonstrated that an increase in photosynthesis results in the rapid growth of microalgae and, consequently, enhances pollutant removal [38,39]. Therefore, we measured the photosynthetic parameters to assess the effect of PAP1 overexpression on the response to OP treatment. As expected, photosynthetic performance (i.e., Fv/Fm, ETR, and NPQ) was higher in *P. tricornutum* cultures overexpressing PAP1 than in the WT strain (Fig. 2). Similarly, as shown in Fig. S4, the transcript level of PAP1 in the OE line was significantly higher than in the WT line and continuously increased throughout the cultivation period. This suggests that PAP1 overexpression significantly increased photosynthesis

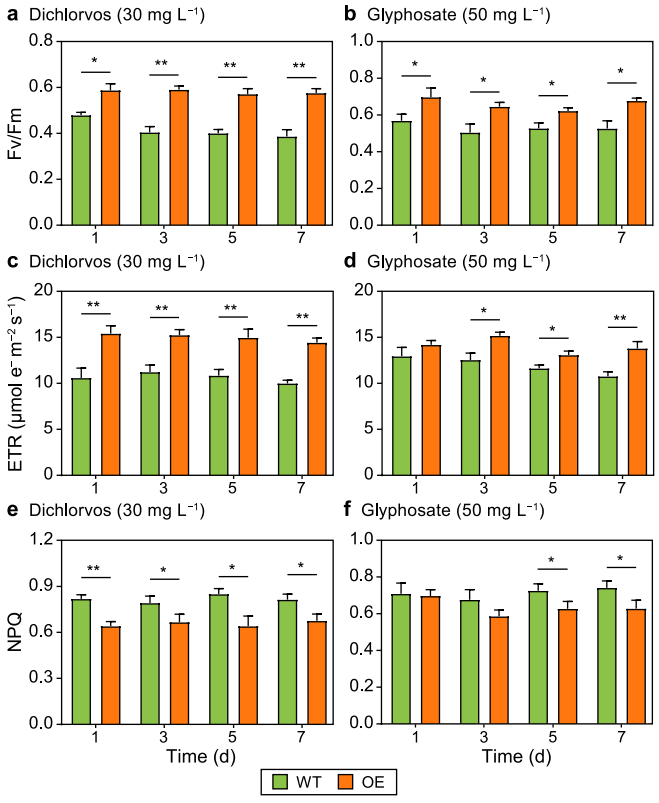

Fig. 2. **a**–**b**, Analyses of the photosynthetic parameters of *P. tricornutum* cultures throughout the cultivation period. Maximum photochemical efficiency of photosystem II (F_v/F_m) in *P. tricornutum* cultures treated with 30 mg L^{-1} dichlorvos (**a**) or 50 mg L^{-1} glyphosate (**b**). **c**–**d**, Electron transport rate (ETR) of *P. tricornutum* cultures treated with 30 mg L^{-1} dichlorvos (**c**) or 50 mg L^{-1} glyphosate (**d**). **e**–**f**, Non-photochemical quenching (NPQ) of *P. tricornutum* cultures treated with 30 mg L^{-1} dichlorvos (**e**) or 50 mg L^{-1} glyphosate (**f**). Each error bar represents the standard deviation of three samples. A significant difference (*$p < 0.05$ and **$p < 0.01$) represents comparisons between the values of the WT and OE lines of *P. tricornutum* cultures.

throughout the cultivation period, thereby resisting and acclimatizing to high concentrations of OPs. However, the photosynthetic parameters of the WT line of *P. tricornutum* continuously decreased in the presence of high concentrations of OPs, indicating the toxicity of OPs to microalgae via irreparable damage to photosynthesis [40].

CO_2 is the primary feedstock required for microalgal photosynthesis; therefore, it is the main factor affecting microalgal biomass production [41]. Previous studies have reported that high CO_2 utilization efficiency may improve the tolerance and biodegradation of organo-pollutants by microalgae [42,43]. Accordingly, the CO_2 utilization efficiency of *P. tricornutum* cultures was determined throughout the cultivation period. As expected, the CO_2 utilization efficiency significantly increased in the presence of PAP1 overexpression (Fig. 3a and b), demonstrating that high CO_2 utilization efficiency may be considered a prerequisite for biomass production and the removal of OPs by *P. tricornutum* cultures. Relevant reports have confirmed that a higher level of CO_2 capture may contribute to photosynthesis by microalgae and, thus, increase biomass accumulation [44]. In addition, effective CO_2 fixation by microalgae has been found to induce pollutant removal [45,46], which agrees with our data. After CO_2 enters microalgal cells, carbonic anhydrase immediately facilitates its fixation to capture excessive CO_2 using a carbon-concentrating mechanism to assist the RuBisCO-mediated Calvin–Benson–Bassham cycle to produce carbohydrates for microalgal growth [47]. Moreover, it has been reported that the positive correlation between carbonic anhydrase and RuBisCO increases photosynthesis, thus enhancing the growth of *P. tricornutum* [48]. As shown in Fig. 3c–f, higher activities of RuBisCO and carbonic anhydrase were observed in the OE line compared with the WT line of *P. tricornutum* cultures, suggesting that excessive CO_2 captured by the OE line to improve CO_2 fixation and photosynthesis efficiency, with the aid of increased RuBisCO and carbonic anhydrase activities, consequently contributed to the simultaneous removal of OPs and accumulation of biomass.

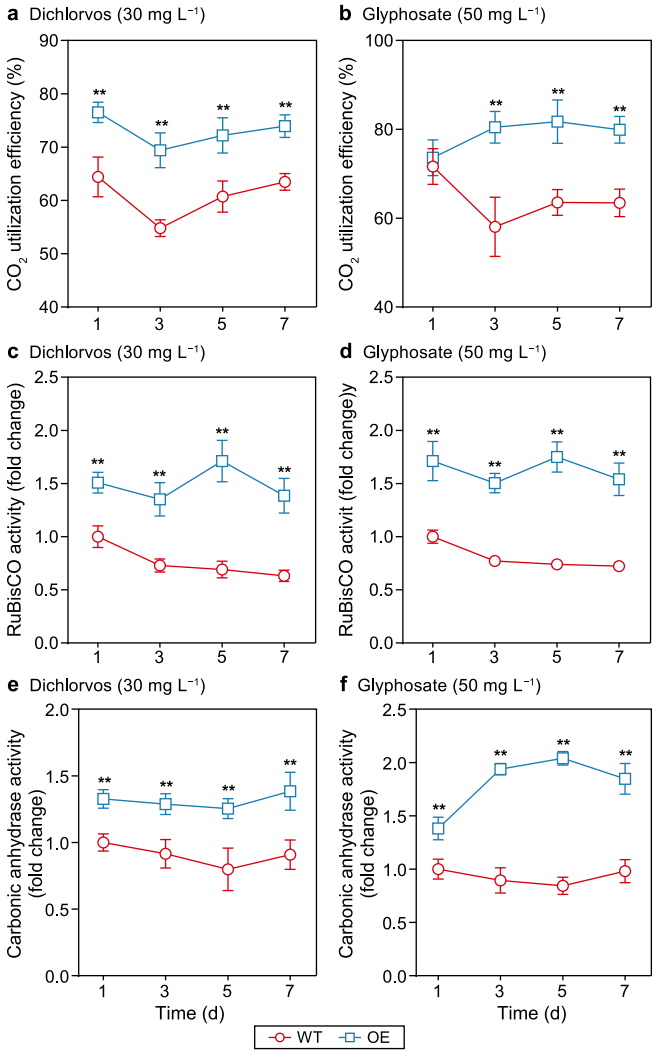

Fig. 3. **a**–**b**, Analyses of the CO_2 utilization and photosynthetic enzymes of *P. tricornutum* cultures throughout the cultivation period. CO_2 utilization efficiency of *P. tricornutum* cultures treated with 30 mg L^{-1} dichlorvos (**a**) or 50 mg L^{-1} glyphosate (**b**). **c**–**d**, Enzymatic activity of ribulose-1,5-bisphosphate carboxylase-oxygenase (RuBisCO) in *P. tricornutum* cultures treated with 30 mg L^{-1} dichlorvos (**c**) or 50 mg L^{-1} glyphosate (**d**). **e**–**f**, Enzymatic carbonic anhydrase activity in *P. tricornutum* cultures treated with 30 mg L^{-1} dichlorvos (**e**) or 50 mg L^{-1} glyphosate (**f**). Each error bar represents the standard deviation of three samples. A significant difference (*$p < 0.05$ and **$p < 0.01$) represents comparisons between the values of the WT and OE lines of *P. tricornutum* cultures.

3.3. The OE line of *P. tricornutum* recalibrated carbon flux into lipid accumulation to improve its biofuel production potential

P. tricornutum is a well-known lipid-producing strain, and historically, it has been considered a biofuel feedstock [49]. Previous studies have also reported that exposure to organic pollutants influences microalgal metabolism, resulting in changes in primary

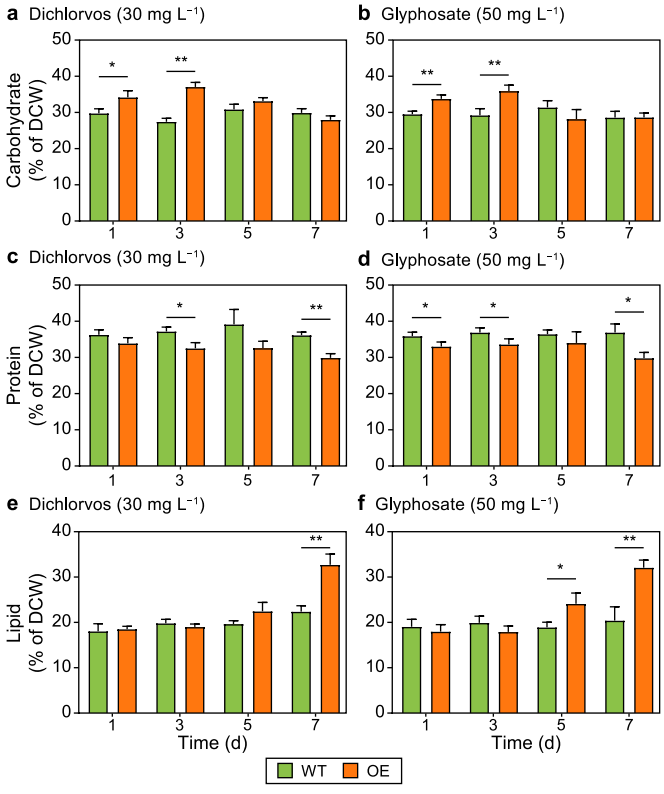

Fig. 4. **a**–**b**, Analyses of primary metabolites of *P. tricornutum* cultures throughout the cultivation period. Carbohydrate content of *P. tricornutum* cultures treated with 30 mg L^{-1} dichlorvos (**a**) or 50 mg L^{-1} glyphosate (**b**). **c**–**d**, Protein content of *P. tricornutum* cultures treated with 30 mg L^{-1} dichlorvos (**c**) or 50 mg L^{-1} glyphosate (**d**). **e**–**f**, Lipid content of *P. tricornutum* cultures treated with 30 mg L^{-1} dichlorvos (**e**) or 50 mg L^{-1} glyphosate (**f**). Each error bar represents the standard deviation of three samples. A significant difference (*$p < 0.05$ and **$p < 0.01$) represents comparisons between the values of the WT and OE lines of *P. tricornutum* cultures.

metabolites [19,29]. As shown in Fig. 4a and b, the carbohydrate content of the OE line was significantly upregulated at the initial cultivation phase (from days 1–4) compared with the carbohydrate content of the WT line of *P. tricornutum* cultures, suggesting that PAP1 overexpression resulted in the accumulation of carbohydrates. This is consistent with the finding that excessive CO_2 capture and sequestration improves photosynthetic performance and, thus, increases carbohydrate biosynthesis [41]. In contrast, the protein content markedly decreased in the OE line compared with the WT line, while the lipid content remained unchanged at the initial cultivation phase (Fig. 4c–f). This demonstrates that the carbon precursor of *P. tricornutum* was allocated towards the biosynthesis of carbohydrates, triggered by the enhanced photosynthetic performance [27]. However, with increasing cultivation time, the lipid content increased due to protein degradation in the OE line of *P. tricornutum* cultures (Fig. 4e and f). This indicates that carbon flux was directed from protein biosynthesis toward lipid biosynthesis. Specifically, lipid was achieved at 32.71% and 32.08% of dry cell weight on day 7 in the engineered strain, which was relatively higher than that reported in previous studies under stress conditions (Fig. 4e and f, Table S2). Similarly, previous studies have demonstrated that the carbon metabolism distribution of microalgae recalibrates to lipid accumulation during the stationary phase [27,29], which is in accordance with our results. Furthermore, the lipid content of the OE line was 32.71% of DCW, which was significantly higher than that of the WT line (22.37% of DCW) when treated with 30 mg L^{-1} dichlorvos (Fig. 4e). On the other hand, the content of total lipids (32.08% of DCW) in the OE line was also remarkably increased compared with that in the WT line (20.42% of DCW) treated with 50 mg L^{-1} glyphosate (Fig. 4f). Previous studies have also demonstrated that the upregulation of lipids during the log phase might be related to the environmental stress treated during the log phase [50,51]. Additionally, the abundance of lipid-related genes in transcripts has been found to play a role in lipid accumulation [28,52]. Consequently, the increase in lipid content on day 5 may correlate with the response to high glyphosate concentration with increasing expression levels of triacylglycerol-related genes. However, the mechanism of lipid content increased on day 5 still needs further investigation. The metabolic response of the OE line of *P. tricornutum* cultures resulting in high lipid accumulation confirmed the rerouting of carbon flux to lipids in the presence of OPs.

The total lipid content of oleaginous microalgae consists of three primary lipogenic components, NL, GL, and PL, which are responsible for membrane structure and energy storage in oleaginous microalgae [53]. Moreover, TAG has been identified as a major component of NL, with an approximate ratio of 90% [52,54]. Accordingly, the fractionated lipid profiles were determined to evaluate the effect of PAP1 overexpressing on the response to treatment with high concentrations of OPs. Interestingly, the NL content of the OE line reached 24.06% and 23.69% after dichlorvos and glyphosate treatment, respectively, significantly higher than the NL content of the WT line (Figs. S5a and b). This agrees with the detected lipid content, shown in Fig. 4e and f, indicating that PAP1 overexpression in *P. tricornutum* cultures triggered an increase in the amount of NL during the biodegradation of OPs. The accumulation of NL at the stationary phase of the OE line of *P. tricornutum* cultures is usually accompanied by TAG biosynthesis, leading to the formation of TAG-rich lipid droplets [52]. In keeping with this observation and similar to the trend of increasing NL content, the TAG content also showed an obvious increase (Figs. S5a and b), confirming that TAG is the main component of NL in oleaginous *P. tricornutum*. However, the GL and PL content of the OE line showed only a slight increase compared with their content in the WT line (Figs. S5a and b). GL is responsible for chloroplast membrane formation [55], which suggests that an increase in GL content accelerates the accumulation of chloroplasts, thereby increasing photosynthetic performance. Furthermore, PL is a crucial component in forming lipid droplets, indicating the positive correlation between PL and TAG content to increase the number of intracellular organelles specialized for storing energy in the form of TAG [56]. Given the considerable lipid accumulation by the OE line of *P. tricornutum*, the mechanistic role of lipogenesis was further examined by measuring the transcript levels of pivotal lipogenic genes. As shown in Fig. S6, the expression levels of *GPAT*, *LPAT*, and *DGAT*, which are involved in TAG biosynthesis, significantly increased after five days of cultivation, indicating that PAP1 overexpression stimulated TAG biosynthesis [26]. These findings collectively indicate that the lipid profile of the OE line was altered in the presence of high concentrations of OPs, indicating its potential as a biofuel feedstock.

The quality of microalgae-based biofuels depends on their thermophysical properties, which are crucial parameters for realistic application as a diesel engine fuel [57]. Furthermore, the biodiesel properties may be affected by the fatty acid methyl esters composition [58]. Therefore, the appropriate ratio of fatty acid methyl esters is a prerequisite to improving the quality of microalgae-based biodiesel for commercial applications [59]. As expected, the total fatty acid content was significantly higher in the OE line than the WT line of *P. tricornutum* by 1.37 and 1.46 times after treatment with high concentrations of dichlorvos and glyphosate, respectively (Fig. S5c). This suggests that PAP1 overexpression triggered the biodegradation of OPs, leading to fatty acid biosynthesis. In addition, the OE line exhibited a remarkable variation in fatty acid composition when treated with high concentrations of OPs (Table S3). The content of saturated fatty acids (SFAs), monounsaturated fatty acids (MUFAs), and polyunsaturated fatty acids (PUFAs) in the OE line was 53.41%, 31.12%, and 15.47% when treated with dichlorvos, and 58.94%, 25.48%, and 15.58% when treated with glyphosate, respectively (Table S3). In particular, the proportions of fatty acids, such as C14:0, C16:0, C18:0, C18:1, C16:3, C18:3, and C20:5, were significantly different in the OE line compared with the WT line after treatment with 30 mg L^{-1} dichlorvos. Meanwhile, after treatment with 50 mg L^{-1} glyphosate, the ratios of C14:0, C16:0, C18:0, C22:0, C16:1, C18:1, C18:3, and C20:5 were significantly affected in the OE line. Changes in the proportion of fatty acids contribute to the alternation of biodiesel properties [58,59]. Therefore, the properties of microalgae-based biofuel important for automotive applications were further assessed in the OE and WT lines of *P. tricornutum* cultures. Interestingly, as shown in Table 1, the primary parameters of microalgae-based biodiesel were found to meet the main requirements of biofuel standards and were consistent with other microalgae-based biofuels. Previous reports have shown that increases in the ratios of specific fatty acids may strengthen the values of ignition quality (given in terms of CN) and OS, thereby improving the quality of microalgae-based biodiesel [60]. Likewise, decreases in CFPP and IV values tend to improve biodiesel performance, with less polymerization and fewer deposits on engines [61]. These results suggest that the biofuels extracted from the OE line of *P. tricornutum* treated with high concentrations of OPs have the potential for use as biofuels.

3.4. Activation of the antioxidant system in the OE line of *P. tricornutum* improved the tolerance and biodegradation of OPs and provided reducing equivalents for lipid accumulation

Pollutant-induced cytotoxicity can trigger excess ROS generation and scavenging, leading to oxidative damage to the microalgae-based metabolic system [62,63]. In contrast, the

Table 1
Comparisons of the properties of biofuels extracted from *P. tricornutum*, based on empirical measurements and calculations, with reference to standards.

Biodiesel properties	Dichlorvos		Glyphosate		Commercial biodiesel	ASTM D7651-08	EN 14214	GB252-2011
	WT	OE	WT	OE				
DU (wt%)	87.87	62.06	85.86	56.64	-	-	-	-
LCSF (wt%)	7.18	4.18	8.09	3.8	-	-	-	-
CFPP (°C)	6.09	−3.36	8.93	−4.52	−5	+5	−5 to −15	-
IV (g I_2 per 100 g)	119.43	78.35	114.6	71.98	130	120 (max)	120 (max)	-
SV (mg KOH)	199.12	207.55	198.52	208.47	-	370 (max)	-	-
CN	46.84	54.97	48.01	56.29	45–55	47 (min)	51 (min)	≥49
KV ($mm^2\ s^{-1}$)	6.75	4.65	5.78	4.73	4	1.9–6.0	3.5–5.0	1.6–9.0
HHV (MJ kg^{-1})	39.47	39.74	39.57	39.8	37.3	40	≤5 or ≤ −20	-
OS (h)	11.79	12.58	11.72	14.08	4	-	≥6	-

Abbreviations: DU, degree of saturation; LCSF, long-chain saturation factor; CFPP, cold-flow plugging point; IV, iodine value; SV, saponification value; CN, cetane number; kV, kinematic viscosity; HHV, high heating value; OS, oxidative stability.

antioxidant system may be activated to eliminate ROS to protect microalgal cells from ROS-induced damage [29]. Therefore, we monitored the ROS level in the microalgae throughout the OP treatment period. The ROS level increased significantly in the WT line during treatment, confirming that OP-induced cytotoxicity caused cellular ROS synthesis (Fig. 5a and b). Interestingly, the ROS level in the OE line was stable and lower than those in the WT line (Fig. 5a and b). This implies that the PAP1 overexpression promoted the elimination of ROS, leading to improved tolerance to OPs. To assess the activation of the antioxidant system, we further investigated the activities of the ROS-scavenging enzymes GPx, SOD, and CAT. The activities of these enzymes continued to significantly increase in the OE line of *P. tricornutum*, compared with those in the WT line, in the presence of very high concentrations of OPs (Fig. S7). Based on the activity levels of the antioxidant enzymes, it was speculated that PAP1 overexpression activated the antioxidant system by increasing the activity of GPx, SOD, and CAT, effectively reducing the effect of cellular ROS. GSH is formed via the reduction of oxidized GSH (GSSG) by the action of reducing equivalents (NADPH) and is involved in the modulation of oxidative stress catalyzed by GPx [64]. Likewise, GSH is considered a pivotal metabolite in detoxifying pollutant-induced cytotoxicity [65,66]. Thus, we determined the GSH/GSSG ratio and the NADPH content in *P. tricornutum* cultures. As expected, the GSH/GSSG ratio was significantly increased in the OE line than the WT line after exposure to OPs (Fig. 5c and d). Due to the increase in GSH levels, the NADPH content was significantly higher in the OE line than in the WT line (Fig. 5e and f). These data suggest that the increased amount of reduced GSH due to NADPH had a significant protective effect against cellular damage caused by exposure to OPs. A previous study demonstrated a positive correlation between GSH synthesis and photosynthesis in the freshwater microalga *Raphidocelis subcapitata* [53]. Thus, we hypothesized that increased GSH activity may be caused by increased NADPH content and photosynthesis, activating the antioxidant system for further detoxification and biodegradation of OPs. Apart from the function of NADPH as a reducing equivalent to form reduced GSH, NADPH is a major source for the biosynthesis of fatty acids and TAG [67]. Similarly, previous reports have demonstrated that the elevated NADPH biosynthesis contributes the alleviation of oxidative damage and also the accumulation of lipid [27,29]. Therefore, we assumed that the increase in NADPH content triggered by OP treatment may also provide essential reducing equivalents for lipid accumulation.

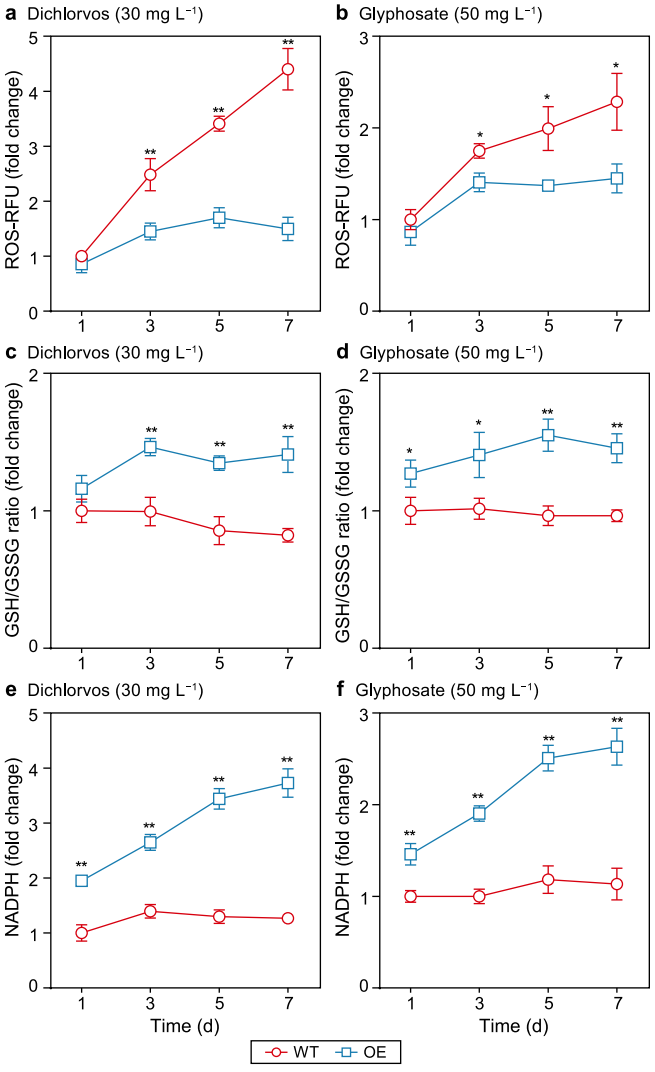

Fig. 5. **a**–**b**, Analyses of primary antioxidant markers of *P. tricornutum* cultures throughout the cultivation period. Relative ROS content of *P. tricornutum* cultures treated with 30 mg L^{-1} dichlorvos (**a**) or 50 mg L^{-1} glyphosate (**b**). **c**–**d**, The GSH/GSSG ratio of *P. tricornutum* cultures treated with 30 mg L^{-1} dichlorvos (**c**) or 50 mg L^{-1} glyphosate (**d**). **e**–**f**, NADPH content of *P. tricornutum* cultures treated with 30 mg L^{-1} dichlorvos (**e**) or 50 mg L^{-1} glyphosate (**f**). Each error bar represents the standard deviation of three samples. A significant difference ($*p < 0.05$ and $**p < 0.01$) represents comparisons between the values of the WT and OE lines of *P. tricornutum* cultures.

3.5. Plausible mechanism for lipid accumulation associated with the highly efficient tolerance and biodegradation of OPs in the OE line of P. tricornutum

OPs are environmentally hazardous compounds that are stable

against hydrolytic degradation. Our investigations excavated that excessive ROS generation was caused by the toxicity of OPs, leading to severe damage to microalgal cells. Similarly, the dysregulation of ROS homeostasis usually causes irreversible oxidative damage to microalgae, initiating the activation of programmed cell death [68,69]. Programmed cell death has been reported to correlate with abnormal levels of biochemical and molecular markers [69,70]. Therefore, we evaluated such markers after initiating the cell death process in response to treatment with OPs. As expected, there was a significant difference in the percentage of PS externalization between the OE line and WT line of *P. tricornutum* (Fig. 6a and b). In particular, the percentage of PS externalization constantly increased in the WT line when exposed to high concentrations of OPs. Furthermore, the percentage of positively PS externalized cells in the OE line was maintained in the 4–7.5% range, much lower than the percentage observed in the WT line. The externalization of PS is a critical marker, as PS is actively translocated to the outer leaflet of the membrane during the cell death process [71,72]. Moreover, caspase-3 activity was simultaneously activated by high concentrations of OPs but was suppressed by PAP1 overexpression in *P. tricornutum* cultures (Fig. 6c and d). The above two biochemical markers were shown to be positively associated with the occurrence of OP-induced programmed cell death, which was in agreement with the results of previous studies [69,72]. Our results imply that PAP1 overexpression may delay the initiation of programmed cell death and maintain microalgal metabolism during OP treatment. The levels of molecular markers (i.e., the transcript abundance of *HSP90*, *DSP*, *MC*, and *PDCD*) exhibited a significant increase along with the upregulated levels of biochemical markers in the WT line of *P. tricornutum* (Fig. 7), suggesting the genetical control of programmed cell death under OP-induced stress. However, the abundance of these transcripts was stable and was significantly restrained as a result of PAP1 overexpression (Fig. 7). Given the biochemical and molecular markers data, a shred of conclusive evidence was provided to elucidate that one potential mechanism for tolerance to OPs in *P. tricornutum* overexpressing PAP1 involved inhibiting programmed cell death through ROS scavenging.

Apart from regulating cellular homeostasis to alleviate the damage caused by OPs, the permeability and potential of the membrane are key features to consider in the diffusion and

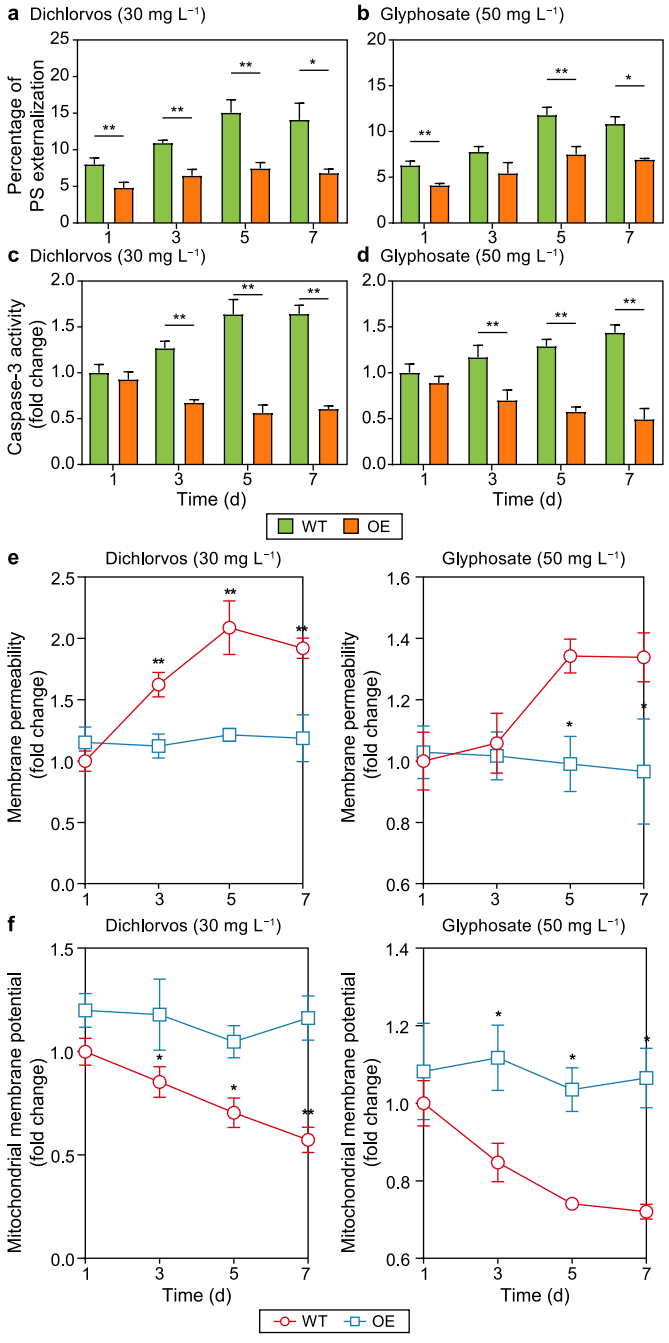

Fig. 6. **a**–**b**, Analyses of primary biochemical markers of programmed cell death in *P. tricornutum* cultures throughout the cultivation period. Percentage of PS externalization of *P. tricornutum* cultures treated with 30 mg L^{-1} dichlorvos (**a**) or 50 mg L^{-1} glyphosate (**b**). **c**–**d**, Caspase-3 activity of *P. tricornutum* cultures treated with 30 mg L^{-1} dichlorvos (**c**) or 50 mg L^{-1} glyphosate (**d**). **e**, Membrane permeability of *P. tricornutum* cultures treated with 30 mg L^{-1} dichlorvos or 50 mg L^{-1} glyphosate. **f**, Mitochondrial membrane potential of *P. tricornutum* cultures treated with 30 mg L^{-1} dichlorvos or 50 mg L^{-1} glyphosate. Each error bar represents the standard deviation of three samples. A significant difference ($*p < 0.05$ and $**p < 0.01$) represents comparisons between the values of the WT and OE lines of *P. tricornutum* cultures.

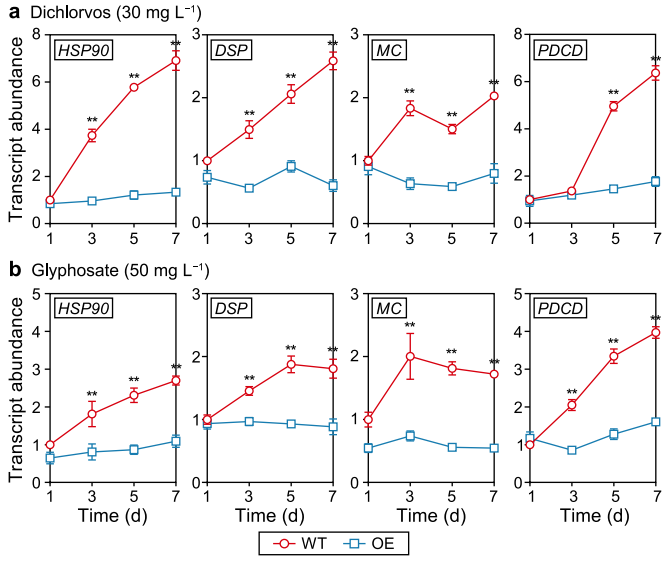

Fig. 7. Analyses of primary molecular markers of programmed cell death in *P. tricornutum* cultures throughout the cultivation period. **a**, Transcript abundances of *HSP90*, *DSP*, *MC*, and *PDCD* genes in *P. tricornutum* cultures treated with 30 mg L^{-1} dichlorvos. **b**, Transcript abundances of *HSP90*, *DSP*, *MC*, and *PDCD* genes in *P. tricornutum* cultures treated with 50 mg L^{-1} glyphosate. Each error bar represents the standard deviation of three samples. A significant difference ($*p < 0.05$ and $**p < 0.01$) represents comparisons between the values of the WT and OE lines of *P. tricornutum* cultures.

metabolism of environmentally hazardous pollutants [73,74]. Notably, the investigation revealed a large difference in membrane permeability between the OE line and WT line (Fig. 6e). These results indicate that PAP1 overexpression mitigated membrane permeability to ameliorate the membrane disruption caused by ROS accumulation [75]. Similarly, mitochondrial membrane potential was substantially enhanced in the OE line compared with the WT line (Fig. 6f). An increase in mitochondrial membrane potential is required for ATP production, which is necessary for cellular metabolism, to improve the tolerance and biodegradation abilities of OPs [29]. It is worthwhile noting that metalloenzymes (e.g., acid phosphatase) exhibit excellent hydrolytic degradation ability for the remediation of organophosphate [76,77]. Similarly, Wang et al. [26] confirmed that PAP1, which has a metal core in its active sites, acts as a pivotal nonspecific phosphomonoesterase in the biodegradation of organophosphates, which subsequently provides sufficient inorganic P for cellular metabolism. As shown in Fig. S4, our data demonstrated a significant increase in PAP1 transcript abundance in the OE line compared with the WT line of *P. tricornutum* cultures. Taken together, these data suggest that PAP1 overexpression enhanced the cellular enzymatic activity of acid phosphatase, leading to an increase in the concentration of inorganic P through the hydrolysis of the phosphoester bond. Based on these data, a plausible mechanism of the increase in enzymatic activity is that OPs biodegraded by overexpressed PAP1 provide sufficient inorganic P for ATP biosynthesis (Fig. 8). The concurrent regulation of carbon flux is anticipated to increase the amount and use of NADPH. Thus, the production of NADPH and ATP may be involved in cellular metabolism to improve OP tolerance and biodegradation competencies by regulating the antioxidant system, delaying programmed cell death, and accumulating lipids via the upregulation of related genes.

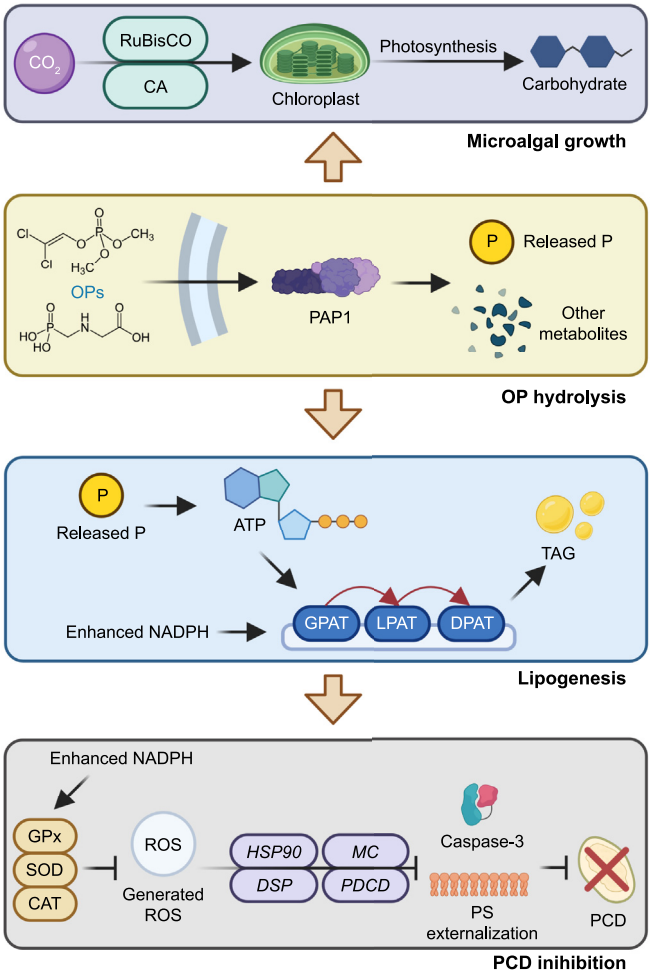

Fig. 8. A plausible mechanism of the OE line of *P. tricornutum* for the OP tolerance and biodegradation competencies, and synergistic biomass and lipid accumulation.

4. Conclusions

In this study, the OE line of *P. tricornutum* was used to treat OPs for the first time. The OE line of *P. tricornutum* exhibited effective competencies for biodegradation of 72.12% and 68.2% for 30 mg L^{-1} of dichlorvos and 50 mg L^{-1} of glyphosate, associated with synergistic accumulations of biomass (0.91 and 0.95 g L^{-1}) and lipids (32.71% and 32.08%), respectively. Moreover, lipids extracted from the OE line after exposure to high concentrations of OPs were found to have favorable biodiesel properties. The activation of the antioxidant system and the inhibition of programmed cell death in the OE line are plausible mechanisms underlying its highly efficient tolerance and biodegradation of OPs, as well as lipid accumulation via the upregulation of related genes. The upscaling treatment of OPs in marine wastewater, associated with their economic and environmental impacts, should be further analyzed to investigate the feasibility of the realistic application. Overall, this study provides novel insights into OP biodegradation and sustainable biofuel production by PAP1-overexpressing *P. tricornutum*.

CRediT authorship contribution statement

Xiang Wang: Conceptualization, Methodology, Data Curation, Writing - Original Draft, Project Administration. **Guo-Hui He:** Methodology, Data Curation, Visualization. **Zhen-Yao Wang:** Methodology, Data Curation. **Hui-Ying Xu:** Methodology, Validation. **Jin-Hua Mou:** Resources, Validation, Investigation. **Zi-Hao Qin:** Resources, Visualization. **Carol Sze Ki Lin:** Writing - Review & Editing, Project Administration. **Wei-Dong Yang:** Resources. **Yalei Zhang:** Writing - Review & Editing. **Hong-Ye Li:** Writing - Review & Editing, Supervision.

Declaration of interests

The authors declare that they have no known competing financial interests or personal relationships that could have appeared to influence the work reported in this paper.

Acknowledgments

This work is funded by the Natural Science Foundation of China (51908244, 31870027), the Guangdong Basic and Applied Basic Research Foundation (2023A1515012314), the China Postdoctoral Science Foundation (2018M643363, 2019T120789) and the Southern Marine Science and Engineering Guangdong Laboratory (Guangzhou) (SMSEGL20SC02).

Appendix A. Supplementary data

Supplementary data to this article can be found online at https://doi.org/10.1016/j.ese.2023.100318.

References

[1] M. Grung, Y. Lin, H. Zhang, A.O. Steen, J. Huang, G. Zhang, T. Larssen, Pesticide levels and environmental risk in aquatic environments in China — a review, Environ. Int. 81 (2015) 87–97.

[2] H. Fu, P. Tan, R. Wang, S. Li, H. Liu, Y. Yang, Z. Wu, Advances in organophosphorus pesticides pollution: current status and challenges in ecotoxicological, sustainable agriculture, and degradation strategies, J. Hazard Mater. 424 (2022) 127494.
[3] A. Amir, A. Raza, T. Qureshi, G.B. Mahesar, S. Jafferi, F. Haleem, M. Ali Khan, Organophosphate poisoning: demographics, severity scores and outcomes from national poisoning control centre Karachi, Cureus 12 (2020) e8371.
[4] V.Y. Tsygankov, Organochlorine pesticides in marine ecosystems of the far eastern seas of Russia (2000–2017), Water Res. 161 (2019) 43–53.
[5] J. Wolfram, S. Stehle, S. Bub, L.L. Petschick, R. Schulz, Meta-analysis of insecticides in United States surface waters: status and future implications, Environ. Sci. Technol. 52 (2018) 14452–14460.
[6] X. Li, S. Jiang, H. Zheng, Y. Shi, M. Cai, Y. Cai, Organophosphorus pesticides in southeastern China marginal seas: land-based export and ocean currents redistribution, Sci. Total Environ. 858 (2023) 160011.
[7] K. Xiao, N. Zhu, Z. Lu, H. Zheng, C. Cui, Y. Gao, Y. Gao, X. Meng, Y. Liu, M. Cai, Distribution of eight organophosphorus pesticides and their oxides in surface water of the East China Sea based on high volume solid phase extraction method, Environ. Pollut. 279 (2021) 116886.
[8] Z. Xie, P. Wang, X. Wang, J. Castro-Jiménez, R. Kallenborn, C. Liao, W. Mi, R. Lohmann, M. Vila-Costa, J. Dachs, Organophosphate ester pollution in the oceans, Nat. Rev. Earth Environ. 3 (2022) 309–322.
[9] J. Kaushal, M. Khatri, S.K. Arya, A treatise on Organophosphate pesticide pollution: current strategies and advancements in their environmental degradation and elimination, Ecotoxicol. Environ. Saf. 207 (2021) 111483.
[10] A. Aswathi, A. Pandey, R.K. Sukumaran, Rapid degradation of the organophosphate pesticide – chlorpyrifos by a novel strain of *Pseudomonas nitroreducens* AR-3, Bioresour. Technol. 292 (2019) 122025.
[11] B. Chen, N. Zhang, S. Xie, X. Zhang, J. He, A. Muhammad, C. Sun, X. Lu, Y. Shao, Gut bacteria of the silkworm *Bombyx mori* facilitate host resistance against the toxic effects of organophosphate insecticides, Environ. Int. 143 (2020) 105886.
[12] H. Mali, C. Shah, D.H. Patel, U. Trivedi, R.B. Subramanian, Degradation insight of organophosphate pesticide chlorpyrifos through novel intermediate 2,6-dihydroxypyridine by *Arthrobacter* sp. HM01, Bioresour, Bioprocess 9 (2022) 31.
[13] T.O. Ajiboye, A.T. Kuvarega, D.C. Onwudiwe, Recent strategies for environmental remediation of organochlorine pesticides, Appl. Sci. 10 (2020) 6286.
[14] W. Zheng, T. Cui, H. Li, Combined technologies for the remediation of soils contaminated by organic pollutants. A review, Environ. Chem. Lett. 20 (2022) 2043–2062.
[15] G. Cao, R. Wang, Y. Ju, B. Jing, X. Duan, Z. Ao, J. Jiang, F. Li, S.H. Ho, Synchronous removal of emulsions and soluble organic contaminants via a microalgae-based membrane system: performance and mechanisms, Water Res. 206 (2021) 117741.
[16] R. Gondi, S. Kavitha, R.Y. Kannah, O.P. Karthikeyan, G. Kumar, V.K. Tyagi, J.R. Banu, Algal-based system for removal of emerging pollutants from wastewater: a review, Bioresour. Technol. 344 (2022) 126245.
[17] X. Hu, Y.E. Meneses, J. Stratton, B. Wang, Acclimation of consortium of microalgae help removal of organic pollutants from meat processing wastewater, J. Clean. Prod. 214 (2019) 95–102.
[18] A.D.M. Satya, W.Y. Cheah, S.K. Yazdi, Y.S. Cheng, K.S. Khoo, D.V.N. Vo, X.D. Bui, M. Vithanage, P.L. Show, Progress on microalgae cultivation in wastewater for bioremediation and circular bioeconomy, Environ. Res. 218 (2023) 114948.
[19] X. Wang, S.F. Liu, Z.H. Qin, S. Balamurugan, H.Y. Li, C.S.K. Lin, Sustainable and stepwise waste-based utilisation strategy for the production of biomass and biofuels by engineered microalgae, Environ. Pollut. 265 (2020) 114854.
[20] X.W. Wang, L. Huang, P.Y. Ji, C.P. Chen, X.S. Li, Y.H. Gao, J.R. Liang, Using a mixture of wastewater and seawater as the growth medium for wastewater treatment and lipid production by the marine diatom *Phaeodactylum tricornutum*, Bioresour. Technol. 289 (2019) 121681.
[21] S. Santaeufemia, J. Abalde, E. Torres, Eco-friendly rapid removal of triclosan from seawater using biomass of a microalgal species: kinetic and equilibrium studies, J. Hazard Mater. 369 (2019) 674–683.
[22] S. Santaeufemia, E. Torres, R. Mera, J. Abalde, Bioremediation of oxytetracycline in seawater by living and dead biomass of the microalga *Phaeodactylum tricornutum*, J. Hazard Mater. 320 (2016) 315–325.
[23] B. Khatiwada, A. Sunna, H. Nevalainen, Molecular tools and applications of *Euglena gracilis*: from biorefineries to bioremediation, Biotechnol. Bioeng. 117 (2020) 3952–3967.
[24] X.J. Lee, H.C. Ong, J. Ooi, K.L. Yu, T.C. Tham, W.H. Chen, Y.S. Ok, Engineered macroalgal and microalgal adsorbents: synthesis routes and adsorptive performance on hazardous water contaminants, J. Hazard Mater. 423 (2022) 126921.
[25] D. Moog, J. Schmitt, J. Senger, J. Zarzycki, K.H. Rexer, U. Linne, T. Erb, U.G. Maier, Using a marine microalga as a chassis for polyethylene terephthalate (PET) degradation, Microb. Cell Fact. 18 (2019) 171.
[26] X. Wang, S. Balamurugan, S.F. Liu, C.Y. Ji, Y.H. Liu, W.D. Yang, L. Jiang, H.Y. Li, Hydrolysis of organophosphorus by diatom purple acid phosphatase and sequential regulation of cell metabolism, J. Exp. Bot. 72 (2021) 2918–2932.
[27] X. Wang, J.H. Mou, Z.H. Qin, T.B. Hao, L. Zheng, J. Buhagiar, Y.H. Liu, S. Balamurugan, Y. He, C.S.K. Lin, W.D. Yang, H.-Y. Li, Supplementation with rac-GR24 facilitates the accumulation of biomass and astaxanthin in two successive stages of *Haematococcus pluvialis* cultivation, J. Agric. Food Chem. 70 (2022) 4677–4689.
[28] S. Balamurugan, X. Wang, H.L. Wang, C.J. An, H. Li, D.W. Li, W.D. Yang, J.S. Liu, H.Y. Li, Occurrence of plastidial triacylglycerol synthesis and the potential regulatory role of AGPAT in the model diatom *Phaeodactylum tricornutum*, Biotechnol. Biofuels 10 (2017) 97.
[29] X. Wang, Z.H. Qin, T.B. Hao, G.B. Ye, J.H. Mou, S. Balamurugan, X.Y. Bin, J. Buhagiar, H.M. Wang, C.S.K. Lin, W.D. Yang, H.Y. Li, A combined light regime and carbon supply regulation strategy for microalgae-based sugar industry wastewater treatment and low-carbon biofuel production to realise a circular economy, Chem. Eng. J. 446 (2022) 137422.
[30] C.F. Hoehamer, C.S. Mazur, N.L. Wolfe, Purification and partial characterization of an acid phosphatase from *Spirodela oligorrhiza* and its affinity for selected organophosphate pesticides, J. Agric. Food Chem. 53 (2005) 90–97.
[31] L.R. Gahan, S.J. Smith, A. Neves, G. Schenk, Phosphate ester hydrolysis: metal complexes as purple acid phosphatase and phosphotriesterase analogues, Eur. J. Inorg. Chem. (2009) 2745–2758, 2009.
[32] H. Tabe, H. Oshima, S. Ikeyama, Y. Amao, Y. Yamada, Enhanced catalytic stability of acid phosphatase immobilized in the mesospaces of a SiO_2-nanoparticles assembly for catalytic hydrolysis of organophosphates, Mol. Catal. 510 (2021) 111669.
[33] T.S. Bhalerao, P.R. Puranik, Microbial degradation of monocrotophos by *Aspergillus oryzae*, Int. Biodeterior. Biodegrad. 63 (2009) 503–508.
[34] Y.H. Zhang, D. Xu, J.Q. Liu, X.H. Zhao, Enhanced degradation of five organophosphorus pesticides in skimmed milk by lactic acid bacteria and its potential relationship with phosphatase production, Food Chem. 164 (2014) 173–178.
[35] X.W. Zhou, X.H. Zhao, Susceptibility of nine organophosphorus pesticides in skimmed milk towards inoculated lactic acid bacteria and yogurt starters, J. Sci. Food Agric. 95 (2015) 260–266.
[36] Q. Liu, X. Wang, J. Zhou, X. Yu, M. Liu, Y. Li, H. Sun, L. Zhu, Phosphorus deficiency promoted hydrolysis of organophosphate esters in plants: mechanisms and transformation pathways, Environ. Sci. Technol. 55 (2021) 9895–9904.
[37] Z. Sarlak, K. Khosravi-Darani, M. Rouhi, F. Garavand, R. Mohammadi, M.R. Sobhiyeh, Bioremediation of organophosphorus pesticides in contaminated foodstuffs using probiotics, Food Control 126 (2021) 108006.
[38] A. Ahirwar, S. Gupta, M. Kashyap, P. Shukla, V. Vinayak, Differential cell viability in *Nitzschia palea* on exposure to different organic and inorganic environmental effluents, Int. J. Environ. Sci. Technol. 17 (1) (2020) 493–504.
[39] M. Xu, D. Ou, Z. Xue, Y. Zhao, S. Sun, J. Liu, Enhancement of the photosynthetic and removal performance for microalgae-based technologies by co-culture strategy and strigolactone induction, Bioresour. Technol. 339 (2021) 125579.
[40] L. Wan, Y. Wu, H. Ding, W. Zhang, Toxicity, biodegradation, and metabolic fate of organophosphorus pesticide trichlorfon on the freshwater algae *Chlamydomonas reinhardtii*, J. Agric. Food Chem. 68 (2020) 1645–1653.
[41] E. Daneshvar, R.J. Wicker, P.L. Show, A. Bhatnagar, Biologically-mediated carbon capture and utilization by microalgae towards sustainable CO_2 biofixation and biomass valorization – a review, Chem. Eng. J. 427 (2022) 130884.
[42] J. Cheng, Y. Zhu, Z. Zhang, W. Yang, Modification and improvement of microalgae strains for strengthening CO_2 fixation from coal-fired flue gas in power plants, Bioresour. Technol. 291 (2019) 121850.
[43] B. Ji, C. Liu, CO_2 improves the microalgal-bacterial granular sludge towards carbon-negative wastewater treatment, Water Res. 208 (2022) 117865.
[44] Z. Arbib, J. Ruiz, P. Álvarez-Díaz, C. Garrido-Pérez, J.A. Perales, Capability of different microalgae species for phytoremediation processes: wastewater tertiary treatment, CO_2 bio-fixation and low cost biofuels production, Water Res. 49 (2014) 465–474.
[45] F. Iasimone, V. De Felice, A. Panico, F. Pirozzi, Experimental study for the reduction of CO_2 emissions in wastewater treatment plant using microalgal cultivation, J. CO_2 Util. 22 (2017) 1–8.
[46] J.Q. Xiong, M.B. Kurade, B.H. Jeon, Can microalgae remove pharmaceutical contaminants from water? Trends Biotechnol. 36 (2018) 30–44.
[47] H. Yu, X. Li, F. Duchoud, D.S. Chuang, J.C. Liao, Augmenting the Calvin–Benson–Bassham cycle by a synthetic malyl-CoA-glycerate carbon fixation pathway, Nat. Commun. 9 (2018) 2008.
[48] X. Zeng, P. Jin, J. Xia, Y. Liu, Correlation of carbonic anhydrase and Rubisco in the growth and photosynthesis in the diatom *Phaeodactylum tricornutum*, J. Appl. Phycol. 31 (2019) 123–129.
[49] T. Butler, R.V. Kapoore, S. Vaidyanathan, *Phaeodactylum tricornutum*: a diatom cell factory, Trends Biotechnol. 38 (2020) 606–622.
[50] F. Han, H. Pei, W. Hu, S. Zhang, L. Han, G. Ma, The feasibility of ultrasonic stimulation on microalgae for efficient lipid accumulation at the end of the logarithmic phase, Algal Res. 16 (2016) 189–194.
[51] M. Takagi, Karseno, T. Yoshida, Effect of salt concentration on intracellular accumulation of lipids and triacylglyceride in marine microalgae *Dunaliella* cells, J. Biosci. Bioeng. 101 (2006) 223–226.
[52] X. Wang, H.P. Dong, W. Wei, S. Balamurugan, W.D. Yang, J.S. Liu, H.Y. Li, Dual expression of plastidial GPAT1 and LPAT1 regulates triacylglycerol production and the fatty acid profile in *Phaeodactylum tricornutum*, Biotechnol. Biofuels 11 (2018) 318.
[53] Y. Zhang, D. He, F. Chang, C. Dang, J. Fu, Combined effects of sulfamethoxazole and erythromycin on a freshwater microalga, *Raphidocelis subcapitata*: toxicity and oxidative stress, Antibiotics 10 (2021) 576.
[54] F. Daboussi, S. Leduc, A. Maréchal, G. Dubois, V. Guyot, C. Perez-Michaut, A. Amato, A. Falciatore, A. Juillerat, M. Beurdeley, D.F. Voytas, L. Cavarec, P. Duchateau, Genome engineering empowers the diatom *Phaeodactylum tricornutum* for biotechnology, Nat. Commun. 5 (2014) 3831.

[55] G. Hölzl, P. Dörmann, Structure and function of glycoglycerolipids in plants and bacteria, Prog. Lipid Res. 46 (2007) 225–243.
[56] H. Goold, F. Beisson, G. Peltier, Y. Li-Beisson, Microalgal lipid droplets: composition, diversity, biogenesis and functions, Plant Cell Rep. 34 (2015) 545–555.
[57] D.C. Rakopoulos, C.D. Rakopoulos, E.G. Giakoumis, Impact of properties of vegetable oil, bio-diesel, ethanol and n-butanol on the combustion and emissions of turbocharged HDDI diesel engine operating under steady and transient conditions, Fuel 156 (2015) 1–19.
[58] M.A. Islam, M. Magnusson, R.J. Brown, G.A. Ayoko, M.N. Nabi, K. Heimann, Microalgal species selection for biodiesel production based on fuel properties derived from fatty acid profiles, Energies 6 (2013) 5676–5702.
[59] P. Chaisutyakorn, J. Praiboon, C. Kaewsuralikhit, The effect of temperature on growth and lipid and fatty acid composition on marine microalgae used for biodiesel production, J. Appl. Phycol. 30 (2018) 37–45.
[60] P. Tamilselvan, L. Sassykova, M. Prabhahar, K. Bhaskar, G. Kannayiram, S. Subramanian, S. Prakash, Influence of saturated fatty acid material composition in biodiesel on its performance in internal combustion engines, Mater. Today: Proc. 33 (2020) 1181–1186.
[61] Y. Huang, F. Li, G. Bao, M. Li, H. Wang, Qualitative and quantitative analysis of the influence of biodiesel fatty acid methyl esters on iodine value, Environ. Sci. Pollut. Res. 29 (2022) 2432–2447.
[62] D. Hu, J. Zhang, R. Chu, Z. Yin, J. Hu, Y. Kristianto Nugroho, Z. Li, L. Zhu, Microalgae *Chlorella vulgaris* and *Scenedesmus dimorphus* co-cultivation with landfill leachate for pollutant removal and lipid production, Bioresour. Technol. 342 (2021) 126003.
[63] L. Míguez, M. Esperanza, M. Seoane, Á. Cid, Assessment of cytotoxicity biomarkers on the microalga *Chlamydomonas reinhardtii* exposed to emerging and priority pollutants, Ecotoxicol. Environ. Saf. 208 (2021) 111646.
[64] J.T. Cirulis, J.A. Scott, G.M. Ross, Management of oxidative stress by microalgae, Can. J. Physiol. Pharmacol. 91 (2013) 15–21.
[65] M.S. Adams, C.T. Dillon, S. Vogt, B. Lai, J. Stauber, D.F. Jolley, Copper uptake, intracellular localization, and speciation in marine microalgae measured by synchrotron radiation X-ray fluorescence and absorption microspectroscopy, Environ. Sci. Technol. 50 (2016) 8827–8839.
[66] S.M. Hamed, M.K. Okla, L.S. Al-Saadi, W.N. Hozzein, H.S. Mohamed, S. Selim, H. AbdElgawad, Evaluation of the phycoremediation potential of microalgae for captan removal: comprehensive analysis on toxicity, detoxification and antioxidants modulation, J. Hazard Mater. 427 (2022) 128177.
[67] J. Xue, Y.F. Niu, T. Huang, W.D. Yang, J.S. Liu, H.Y. Li, Genetic improvement of the microalga *Phaeodactylum tricornutum* for boosting neutral lipid accumulation, Metab. Eng. 27 (2015) 1–9.
[68] S. Zhang, C.B. Qiu, Y. Zhou, Z.P. Jin, H. Yang, Bioaccumulation and degradation of pesticide fluroxypyr are associated with toxic tolerance in green alga *Chlamydomonas reinhardtii*, Ecotoxicology 20 (2011) 337–347.
[69] Y. Zhao, X. Tang, F. Qu, M. Lv, Q. Liu, J. Li, L. Li, B. Zhang, Y. Zhao, ROS-mediated programmed cell death (PCD) of *Thalassiosira pseudonana* under the stress of BDE-47, Environ. Pollut. 262 (2020) 114342.
[70] H. Wang, F. Chen, T. Mi, Q. Liu, Z. Yu, Y. Zhen, Responses of marine diatom skeletonema marinoi to nutrient deficiency: programmed cell death, Appl. Environ. Microbiol. 86 (2020) e02460-02419.
[71] K.D. Bidle, The molecular ecophysiology of programmed cell death in marine Phytoplankton, Ann. Rev. Mar. Sci 7 (2015) 341–375.
[72] K.D. Bidle, Programmed cell death in unicellular Phytoplankton, Curr. Biol. 26 (2016) R594–R607.
[73] S. Hena, L. Gutierrez, J.P. Croué, Removal of pharmaceutical and personal care products (PPCPs) from wastewater using microalgae: a review, J. Hazard Mater. 403 (2021) 124041.
[74] Y. Yu, Y. Zhou, Z. Wang, O.L. Torres, R. Guo, J. Chen, Investigation of the removal mechanism of antibiotic ceftazidime by green algae and subsequent microbic impact assessment, Sci. Rep. 7 (2017) 4168.
[75] A.J.S. Al-Azab, D. Widyaningrum, H. Hirakawa, Y. Hayashi, S. Tanaka, T. Ohama, A resin cyanoacrylate nanoparticle as an acute cell death inducer to broad spectrum of microalgae, Algal Res. 54 (2021) 102191.
[76] C. Pathak, S.K. Gupta, M.K. Gangwar, A.P. Prakasham, P. Ghosh, Modeling the active site of the purple acid phosphatase enzyme with hetero-dinuclear mixed valence M(II)–Fe(III) [M = Zn, Ni, Co, and Cu] complexes supported over a [N_6O] unsymmetrical ligand, ACS Omega 2 (2017) 4737–4750.
[77] L.F. Serafim, L. Wang, P. Rathee, J. Yang, H.S.F. Knaul, R. Prabhakar, Remediation of environmentally hazardous organophosphates by artificial metalloenzymes, Curr. Opin. Green Sustainable Chem. 32 (2021) 100529.